LOW-DENSITY GAS DYNAMIC FACILITY

Thesis by

James A. McGill

Lieutenant Commander

United States Navy

In Partial Fulfillment of the Requirements

For the Degree of

Aeronautical Engineer

California Institute of Technology

Pasadena, California

1967

(Submitted September 22, 1966)

ACKNOWLEDGMENTS

The author is grateful to Dr. Frank E. Marble, for stimulating the initial interest in this subject; to Dr. Edward E. Zukoski, for his guidance and generous help; and to Dr. Hans W. Liepmann, for use of the vacuum vessel which he designed and used to investigate orifice flow.

Thanks are also due to the United States Navy for its postgraduate education program; to Mr. Frank T. Linton, for aiding in the construction of the facility and preparation of the graphical figures; to Mrs. Roberta Duffy, for typing the manuscript; to my wife, Dagmar, for typing the rough draft and helping me to survive the darkest hours; and last, but not least, to LT Arnold H. Henderson, my cohort.

ABSTRACT

The question of optimizing nozzle contours for micro-thrust rockets led to the design, construction, and testing of a low-density gas dynamic facility. The primary objective was to investigate the mass flow rates of a gas through various profiles in the slip and transition flow regimes at high pressure ratios.

An initial test was conducted with an orifice as the test profile. The results showed that the facility can be used to investigate mass flow rates from the threshold of the free-molecule, through the transition and slip, to the continuum regimes. These results compare favorably with those of two previous investigators, and asymptotically approach the theoretical continuum and free-molecule limits. The ratio of mass flow rate to theoretical free-molecule mass flow rate is shown to transition smoothly from one theoretical limit to the other. A local maximum may occur in this ratio in the slip regime, and the attainment of the theoretical free-molecule limit appears to occur more slowly than expected.

TABLE OF CONTENTS

LIST OF SYMBOLS

a	molecular collision diameter
c	mean molecular speed
d	aperture diameter
f	transfer ratio of momentum
g	gravitational constant
h	height difference
k	constant
$\dot{m}$	mass flow rate
n	molecule number density
p	pressure
r	cylindrical or spherical radius
u	axial velocity
v	volume
x	axial coordinate
A	area
C	discharge coefficient
F	collision frequency per mole
H	perimeter
K	Boltzmann constant
Kn	Knudsen number
M	molecular weight
Ma	Mach number
N	number of molecules striking a unit area of wall per unit time
P	pressure

Q	volumetric flow rate
R	specific gas constant
Re	Reynolds number
T	temperature
V	volume
W	characteristic velocity
Z	empirical coefficient
α	orifice discharge coefficient
γ	ratio of specific heats
ζ	coefficient of slip
θ	spherical elevation angle or conical half angle
λ	mean free path
μ	viscosity
ν	kinematic viscosity
ρ	density
ϕ	spherical azimuth angle
Γ	dimensionless flow function
$\varkappa$	Clausing factor
$( )_c$	stagnation chamber or upstream
$( )_e$	exhaust chamber or downstream
$( )_f$	float
$( )_{fm}$	free-molecule
$( )_k$	free-molecule
$( )_w$	fluid

I. INTRODUCTION

The flow of gases can be roughly divided into four regimes characterized by the Knudsen number (Kn), the ratio of molecular mean free path to a characteristic length in the flow field. These four regimes are:

continuum flow	$\sim$	$Kn < 0.01$
slip flow	$\sim$	$0.01 < Kn < 0.1$
transition flow	$\sim$	$0.1 < Kn < 1$
free-molecule flow	$\sim$	$5 < Kn$

The Navier-Stokes equations with appropriate boundary conditions describe the flows in the continuum and slip flow regimes while the kinetic theory of gases must be used in the transition and free-molecular regions.

For flows through orifices, nozzles,and short tubes well into the continuum regime, the boundary layers on the walls usually represent only a very small portion of the flow field. These boundary layers become more and more dominant as the Knudsen number increases, until they occupy the entire flow field at large Knudsen numbers. In the slip regime, the boundary layers no longer have zero velocity at the walls. In free-molecule flow,collisions between gas molecules can be neglected compared with collisions between gas particles and the body. In such cases, the fluxes of incident and reflected particles can be treated separately. In the transition regime where the mean free path and the characteristic dimension of the body are of the same order of magnitude, both intermolecular collisions and molecule-surface interactions must be considered. In

order to obtain experimental data for a better understanding of the transition from continuum to free-molecule flow, the present low-density gas dynamic facility was designed and built.

The initial interest in this area of low-density gas flow was generated by the problem of nozzle contours for micro-thrust rocket motors. In these rockets with extremely low thrust, the exhaust gases are in the flow regime between continuum and free-molecule. The optimization of these nozzle contours depends upon having some basic knowledge of gas flow in the slip and transition regimes. It is hoped that this low-density gas dynamic facility will supply some basic experimental data about slip and transition flow through various contours.

II. APPARATUS

General Description

The low-density gas dynamic facility is a continuous flow, open-circuit type designed to operate with stagnation chamber pressures of from 1 μ to $\frac{1}{2}$ atm and exhaust chamber pressures to give at least a 100:1 pressure ratio across the test section.

Figure 1 is a photograph of the facility; subsystems are shown schematically in Figures 2 - 4. The pumping system consists of a 300-cfm rotary pump, Stokes Model 412-H, in parallel with a 2-in. metal-oil fractionating diffusion pump, CVC Model PMCS-2C, backed by a 7-cfm rotary pump, Cenco Hypervac 25 (Figure 4). The pumping characteristics as supplied by the manufacturers are shown in Figures 5 and 6.

The vacuum vessel (Figure 3) is a cylindrical steel chamber of about 40-cm internal diameter and 90-cm length. The tank is divided into the stagnation and exhaust chambers by a central bulkhead which contains a cutout for mounting a machined test profile plate. For rapid pump-down, a bypass is incorporated around the test section. The tank has provisions for three stagnation-chamber pressure taps. The exhaust chamber pressure line enters the chamber through the 4-in. outlet and extends about half way into the chamber. The tip of the pressure line is off to the side of, and turned at a right angle to, a direct line between the test section and the outlet. Access to the test section is gained through an O-ring-sealed plate in the inlet side of the stagnation chamber. This plate

incorporates the inlet line and one pressure tap.

Test Gas Feed and Measurement

The test gas is fed from a standard gas bottle through first, a 25- to 650-psig high-pressure regulator, Matheson Model 2, and then, a 3- to 15-in. water-column low pressure regulator, Matheson Model 70 B, before passing to a liquid-nitrogen cold trap. From the cold trap, the gas flows through a constant-temperature water bath to the flow measurement system. At the inlet to the flow measurement system, there are both pressure and temperature taps. The pressure line is connected to a 0- to 15-psia dial gauge, Burton Model 2311-001 and a 0- to 800-mm mercury manometer, Wallace and Tiernan Model FA 135, and the temperature tap houses a precision mercury thermometer, ASTM-Saybolt Viscosity Thermometer 17F (66° to 80° F). The pressure gauge can be read to within ± 0.01 psia and is accurate to within $\frac{1}{2}$ per cent full scale. The thermometer can be read to within ± 0.05° F.

The flow measurement system consists of two subsystems of different flow measuring devices (Figure 2). The first is a parallel array of four rotameters, Brooks Models R-2-15-AA with stainless steel float, R-2-25-D, R-2-25-A, and R-2-25-B with sapphire floats. These four rotameters are capable of measuring helium flow over the ranges 0.4 to 4.3, 1.0 to 10.9, 4.0 to 36, and 10 to 108 cc/sec at 760 mm Hg and 70° F. The rotameters were calibrated by the author after they were installed in the facility by the water displacement method at atmospheric conditions. Each calibration

curve is based on at least 20 data points that are reproducible to within ± 1 per cent from 30 to 100 per cent of full-scale reading. The overlapping range of adjacent rotameters permits each meter to be used in its upper, more accurate, range (Figure 7).

The governing equation for a rotameter is:

$$Q = A_w C \left[\frac{2gV_f(\rho_f - \rho_w)}{A_f \rho_w} \right]^{\frac{1}{2}} \qquad (1)$$

where

Q = volumetric rate of flow,

V_f = volume of float,

g = gravitational constant,

ρ_f = float density,

ρ_w = fluid density

A_f = area of float,

C = discharge coefficient,

A_w = area of annular orifice, $= \frac{\pi}{4}[(D+by)^2 - d^2]$,

D = effective diameter of tube depending on position of float,

b = change in tube diameter per unit change in height,

d = maximum diameter of float, and

y = height of float above zero position.

The value of C is a weak function of Reynolds number, but through careful design, the effect is largely eliminated for certain ranges of Reynolds number. Thus, when the rotameter is calibrated and used for a single fluid at approximately the same conditions of temperature

and pressure, C may be taken as a constant.

For a gas ρ_w is negligible compared with ρ_f, so equation (1) becomes

$$Q = A_w C\left[\frac{2gV_f\rho_f}{A_f\rho_w}\right]^{\frac{1}{2}} . \qquad (2)$$

Therefore, for any given position of the float $Q = k\rho_w^{-\frac{1}{2}}$ where k is a constant[1].

Once the meter is calibrated at known conditions of temperature and pressure for a given gas, the reading can be interpreted at other (not greatly different) conditions for the same gas by knowing the gas densities or equation of state:

$$Q = Q_c\left(\frac{\rho_{wc}}{\rho_w}\right)^{\frac{1}{2}} = Q_c\left(\frac{P_c}{P}\,\frac{T}{T_c}\right)^{\frac{1}{2}} \qquad (3)$$

where the subscript c stands for the calibration condition. The mass flow rate ($\dot{m}$) therefore can easily be determined:

$$\dot{m} = Q\rho_w = Q_c(\rho_{wc}\rho_w)^{\frac{1}{2}} . \qquad (4)$$

The second flow measurement subsystem is a Brooks Vol-U-Meter. This is a precision-bore, vertical borosilicate glass tube containing a polyvinylchloride floating piston having a mercury O-ring seal. The usable length of the tube is 30 in. and the internal volume is indicated every 1 cc from 0 to 25 cc. The precision of the instrument is 0.2 per cent of indicated volume. By measuring the time required for the piston to rise through a given displacement and knowing the output pressure and temperature, the mass flow rate can be calculated. Volume flow rates from about 0.003

to 2. 5 cc/sec can be measured, the lower end being limited only by the patience of the operator and the overall stability of the system, and the upper end by the reaction time of the operator and the difficulty in gauging when the piston passes a given volume mark.

It was found that the test gas stays at room temperature throughout the facility after it has passed through the water bath at room temperature. Thus, the temperature at the input to the flow measuring system is taken as the temperature in the Vol-U-Meter. A pressure tap is installed in the output line of the Vol-U-Meter. This pressure is indicated on a 0 to 25- and 25 to 50-psig dual-range dial gauge, Wallace and Tiernan Model FA233111, and is taken as the pressure in the Vol-U-Meter. It was found that the pressure drop across the mercury-sealed piston was about 0. 08 psi, or less than 1 per cent of the input pressure.

During runs in which the Vol-U-Meter is to be used, the Vol-U-Meter is bypassed until a steady-state condition is attained. Once steady-state is established, the Vol-U-Meter bypass is closed and the test gas is drawn from the Vol-U-Meter until the flow rate has been determined. Once this has been accomplished, the bypass is again opened. The steady-state conditions are checked before, during, and after the volumetric measurement in order to be certain that the stagnation chamber remains at the same steady-state condition.

From the flow measurement system, the test gas is fed to the stagnation chamber through a variable leak, Granville-Phillips Series 203. This variable leak is used to control the test-gas flow

rate, and thus the pressure in the stagnation chamber. The conductance of the variable leak is continuously variable from approximately 100 to 10^{-10} cc/sec with atmospheric pressure on the inlet side and vacuum on the outlet. Fully-closed conductance is stated by the manufacturer to be less than 10^{-13} cc/sec. Twenty-seven full turns of the driver handle provides precise control over the entire conductance range. A counter, graduated in units corresponding to 1/10 turn of the handle, is helpful in setting approximate conductances. At the higher flow rates and stagnation chamber pressures, a given setting gives reproducible performance. At the lower settings, hysteresis losses found in all devices with metal-to-metal seals cause slight variations in performance at any given setting. Figure 8 shows approximate counter setting versus stagnation chamber pressure over the range of 0.01 to 200 mm Hg.

Test Profile Plate

The test profiles are machined in steel plates which are fitted with O-ring seals into a cut-out in the dividing bulkhead of the vacuum vessel. The stagnation chamber side of the plates is flush with the surface of the dividing bulkhead so that no undue entrance effects are present. The minimum diameter of the test profile is approximately 1 mm. Thus, the ratio of tank diameter to profile diameter is about 400 to 1. For all practical purposes, the stagnation and exhaust chambers are of infinite size in comparison with the test profile. Therefore, the effects of the tank walls on the flow field through the test profile are negligible.

The first profile tested was a sharp-edged orifice with a diameter of 0.039 in. and an edge thickness of 0.0035 in. (Figure 9). Subsequent profiles will be short tubes and conical profiles of various entrance and exit half angles.

Pump System

The 4-in. outlet of the exhaust chamber is connected to a welded aluminum tee. The tee has 4- and 2 1/4-in. flanged outlets. Both the outlets are fitted with handwheel-operated gate valves, Temescal Series 5000. From the 4-in. valve the flow drops 12 in. in a flanged Zee connector which serves as a baffle to prevent backflow of oil from the Stokes pump. The Stokes pump is vibration isolated from the Zee connector by means of a 6-in. stainless steel bellows. The exhaust of the Stokes pump is vented outside the building (Figure 1).

The 2 1/4-in. Temescal valve is connected by O-ring seals to the input flange of the CVC diffusion pump. The exhaust of this pump is fed to the Cenco rotary backing pump by means of 1-in. diameter copper tubing that is isolated from the diffusion pump by means of a short piece of Tygon tubing (Figure 1).

This pumping arrangement permits rapid pump-down of the system to the micron range by use of the Stokes pump. The pump-down time to 10 μ is approximately one minute (Figure 10). The diffusion pump can be isolated from the system and warmed to operating conditions while the Stokes pump is exhausting the system. The switch-over to the diffusion pump is accomplished without any

increase in system pressure by simply opening the 2 1/4-in. Temescal valve and closing the 4-in. valve. It has been the practice to keep the diffusion pump in continuous operation and simply isolating it from the system when the flow rate and exhaust chamber pressures are such as to dictate the use of the Stokes pump as the primary vacuum source.

Vacuum Pressure Measurement

The primary means of measuring vacuum pressure is a bank of two McLeod gauges, made by Greiner Glassblowing Laboratory, a 0- to 800-mm mercury manometer, Wallace and Tiernan Model FA 135, and a 0- to 50-mm dial gauge, Wallace and Tiernan Model FA 160. One McLeod gauge is a non-linear gauge that measures the range 0 to 125 μ on a 230-mm scale and that has a capture volume of 330.6 cc. The second, linear gauge, has three 500-mm scales that measure the ranges 0 to 1, 0 to 10, and 0 to 100 mm with a capture volume of 250.5 cc.

In the non-linear gauge, a known volume of sample gas at the unknown pressure is captured and then compressed in a 1-mm capillary that is sealed at its upper end until a reference column of mercury in a similar capillary is even with the end of the sealed capillary. The difference in the heights of the mercury columns in the two capillaries is then a measure of the unknown pressure. Assuming isothermal compression, the following holds:

$$PV = pv \tag{5}$$

where

P = unknown pressure,

V = capture volume,

p = pressure in the compressed volume,

v = compressed volume; and

$$v = Ah \tag{6}$$

where

A = capillary cross-sectional area, and

h = difference in height of mercury in the two capillaries.

With

$$p = P + h \quad \text{(all pressures in mm Hg)}, \tag{7}$$

$$P = \frac{pv}{V} = (P+h)\frac{Ah}{V}$$

from equations (5) - (7).

In the micron range, $P \ll h$, so that equation (8) becomes

$$P = \frac{Ah^2}{V} = kh^2 \ , \tag{9}$$

where k = known constant.

In the linear gauge, a known volume is captured and then compressed to one of three known volumes. The height of a column of mercury above the compressed reference volume is then a measure of the original unknown pressure. Assuming the isothermal relation again, $PV = pv$; however, here v is the known reference volume; then

$$P = (P+h)\frac{v}{V} \tag{10}$$

$$P = h\left(\frac{1}{V/v - 1}\right) \tag{11}$$

$$P = kh \tag{12}$$

where k is a known constant.

CVC GTC 100 thermistor gauges are used to monitor the stagnation and exhaust chamber pressures. These are used to indicate pressure variations in the tank and to check on the attainment of steady conditions, but are not used as a primary means of pressure measurement.

III. THEORY

The flow of a gas through orifices, short tubes, and nozzles at high pressure ratios in the slip and transition regimes involves spanning the gap between gas dynamics and gas kinetics. At both ends of this spectrum, the governing equations and boundary conditions are well defined, although solutions to the flow problem may not be readily obtainable. For slip flow, the governing equations are the Navier-Stokes equations, but the boundary conditions are not known. The conditions at the wall of an object are no longer the zero velocity conditions of continuum flow. In the transition regime, the governing equations would seem to be those of gas kinetics, but account must be taken of intermolecular as well as molecule-surface collisions.

Continuum Flow

Far into the continuum regime where boundary layers occupy only a small portion of the flow field, the flow problem can be analyzed to a good degree of approximation by assuming an inviscid flow field. In this region, there exists a definite critical pressure ratio (P_c/P_e) beyond which the downstream conditions cease to influence the upstream conditions. The maximum mass flow is reached at this critical pressure ratio for given upstream conditions. For a smooth nozzle, this condition is reached when the Mach number is unity at the throat, since the maximum mass flow density occurs at local sonic velocity. This maximum pressure ratio and corresponding mass flow are:

$$\frac{P_c}{P_e} = \left(\frac{\gamma+1}{2}\right)^{\frac{\gamma}{\gamma-1}} \tag{13}$$

$$\dot{m} = \rho A V = \frac{P_c}{\sqrt{T_c}}\sqrt{\frac{\gamma}{R}}\left[\frac{2}{\gamma+1}\right]^{\frac{1}{2}\frac{\gamma+1}{\gamma-1}} A$$

$$= \rho_c A(\gamma R T_c)^{\frac{1}{2}} \left(\frac{2}{\gamma+1}\right)^{\frac{1}{2}\frac{\gamma+1}{\gamma-1}} . \tag{14}$$

Although this choked condition gives the maximum mass flow, it does not determine the nature of the flow downstream of the throat which is essential to optimization of a nozzle. For this analysis, the methods of one-dimensional isentropic flow or characteristics can be used. In these analyses, the boundary layers on the walls can usually be neglected to a good approximation. When they are taken into account, it is usually as a small correction to the nozzle area based upon the boundary-layer displacement thickness.

As the slip regime is approached, the boundary layers play a more important role in determining the over-all flow. Eventually they fill the entire nozzle, and the gas flow is more like fully-developed laminar flow in a long tube than conventional nozzle flow. Marble has done a preliminary analysis which

> "attempts to treat the low Reynolds number nozzle problem by modifying the formulation to include the viscous stresses associated with wall shear, but neglecting the normal viscous stress associated with acceleration along the flow direction. It is assumed that the flow is dissipative, but locally adiabatic. Under these restrictions the results should be adequate to indicate the order of magnitude of the losses and of their effects on nozzle geometry." [2]

In this analysis, the velocity dependence on axial distance along the nozzle is chosen. This, together with the gas thermodynamic properties and an estimate of the cross-sectional velocity profile, yields the information required to estimate the nozzle geometry to achieve a given nozzle performance. Marble concludes that viscous dissipation plays a strong role for small Reynolds numbers, and that for a given mass flow, as the length of the nozzle is increased, the area ratio must increase to achieve the same discharge velocity. For very low Reynolds numbers, the nozzle divergence angle must be increased as the length is increased. [2]

Although the choked condition for a nozzle in continuum flow occurs at modest pressure ratios (P_c/P_e = 1.89 for air and 2.06 for He), much higher ratios are required for the flow through an orifice. This is because the sonic line for an orifice is S-shaped, while that of the nozzle is planar. Since the flow in the plane of the orifice is not sonic, it follows that the mass flow is smaller than for a smooth nozzle of the same throat area.

The two-dimensional analogy to orifice flow, flow through a slit, has been analyzed by the method of characteristics[3]. The flow becomes sonic at the lip of the slit and flows locally around the lip like a Prandtl-Meyer expansion. The streamline maps on a characteristic in the hodographic plane. When the characteristic connects the sonic point on the axis with the corner, the flow downstream has no effect on the upstream conditions and the flow is choked. This characteristic is an epicycloid from the sonic circle on

the u-axis and meets the corner characteristic at $\theta = 45^{o}$. The critical pressure ratio is the one corresponding to this 45^{o} turn from sonic in Prandtl-Meyer flow. Liepmann gives the critical pressure ratios as 58.3, 25.6, and 21.5 for γ's of 5/3, 7/5, and 4/3, respectively[4].

Obtaining the mass flow is more difficult, for the full hodograph equation must be solved. Frankl has computed for a two-dimensional slit that the ratio of the mass flow to the mass flow of a smooth nozzle of equal area is 0.85 for a gas with $\gamma = 1.4$.[5]

The axisymmetric problem of the orifice is even more difficult since the hodograph equations are not linear. Liepmann gives an argument that shows that the required Prandtl-Meyer turning angle and pressure ratio are larger for an orifice while the mass flow is smaller than for a slit. The differences between the two should be small. Thus, it is expected that the mass flow through an orifice at high Reynolds number will be:

$$\dot{m} = \alpha \frac{P_c}{\sqrt{T_c}} \sqrt{\frac{\gamma}{R}} \left[\frac{2}{\gamma+1}\right]^{\frac{1}{2}\frac{\gamma+1}{\gamma-1}} A \ , \qquad (15)$$

where α is on the order of 0.85.[4]

As the Reynolds number is decreased, boundary layers build up near the lip and into the orifice. These can have two effects. First, they reduce the effective area of the orifice, and second, they can round out the orifice entrance and tend to increase the mass flow. Liepmann[4] states that a limiting formula at high Reynolds number should have the form

$$\dot{m} = \dot{m}_{Re>\infty}(1 - CRe^{-\frac{1}{2}}) \tag{16}$$

where C is a constant. He states that experimentally C is of the order of $\frac{1}{2}$.

The third profile of interest, the short tube, would be expected to act similarly to an orifice in the continuum regime with the same entrance and boundary layer effects.

Free-Molecule Flow

In the free-molecule regime, where the mean free path is much larger than the characteristic dimension of the profile in question, the flow through the profile can be determined by the methods of kinetic theory. It is a matter of statistically keeping track of molecules and their surface interactions.

Following Present[6], one can compute the number of molecules passing through an orifice. Consider an element of area on the wall dA. Choose a system of spherical coordinates with origin at the center of dA and axis normal to dA. The mean free path of the gas molecules is

$$\lambda = \frac{KT_c}{\sqrt{2}\, P_c \pi d^2} = \frac{n}{\sqrt{2}\, \pi a^2} \quad . \tag{17}$$

The mean molecular velocity is

$$c = \sqrt{(8/\pi)\, RT_c} \quad . \tag{18}$$

The collision frequency per molecule is

$$F = \sqrt{2}\, \pi a^2 cn \tag{19}$$

where n = molecule number density and a = collision diameter. The number of molecule collisions in a volume element dv located at r , θ , and ϕ is equal to the average number of molecules in dv times the probability per unit time that a molecule collides,

$$ndvF = (c/\lambda)ndv \quad . \tag{20}$$

Molecules leave dv in random directions. The fraction that leaves dv in the direction of dA is $dA|\cos\theta|/4r^2$. The fraction of molecules leaving dv toward dA which arrive at dA without undergoing further collisions is

$$\frac{cndv}{\lambda} \frac{dA|\cos\theta|}{4\pi r^2} e^{-r/\lambda}$$

where $e^{-r/\lambda}$ is the probability that a molecule travels a distance r , from its last collision, without a further collision. The total number of molecules striking a unit area of wall per unit time is

$$N = \frac{cn}{4\pi\lambda} \iiint \frac{|\cos\theta|}{r^2} e^{-r/\lambda} dv \tag{21}$$

$$= \frac{cn}{4\pi\lambda} \int_0^{2\pi} d\phi \int_0^{\pi/2} d\theta \sin\theta \cos\theta \int_0^{\infty} dr\, e^{-r/\lambda}$$

$$= \frac{nc}{4} \quad . \tag{22}$$

Now, consider a small hole of diameter d much smaller than the mean free path. A molecule in the vicinity of the hole and traveling toward it will pass through the hole without suffering any collision in the neighborhood. The molecules pass through individually and independent of the motion of other molecules[6].

Equation (22) gives the number flow of molecules through a sharp-edged orifice when the Knudsen number is sufficiently high. It can be applied to the gas on both sides of the orifice to give the net flow, since the two flows are independent of each other if the mean free paths on each side of the orifice are much larger than the diameter. This type of flow is called effusive flow or effusion. If the gas on each side of the orifice is at the same temperature, the net mass flow rate is therefore

$$\dot{m} = \frac{1}{\sqrt{2\pi RT}} A(P_c - P_e) \tag{23}$$

where

A = area of the orifice,

P_c = upstream pressure,

P_e = downstream pressure.

When the orifice is not sharp-edged but has a finite length, some of the molecules collide with the side walls of the orifice and then are re-radiated in a random fashion. This causes some of the molecules that enter the orifice, or short tube, to be re-emitted to their original side of the orifice. Clausing showed that the correct expression for circular cross-sections is

$$\dot{m} = \frac{\varkappa}{\sqrt{2\pi RT}} A(P_c - P_e) \tag{24}$$

where $\varkappa$ is a function of the length-to-diameter ratio of the orifice or tube and is called the Clausing factor. As the tube becomes long, $\varkappa$ approaches $4d/3\ell$ as an upper limit.[7] Present gives a derivation for the mass flow for long tubes and shows that $\varkappa = 4d/3\ell$ from geo-

metric and gas kinetic considerations[6].

For long tubes of varying cross section A and perimeter H, the fundamental relation deduced by Knudsen is (cs. refs. 7, 8)

$$\dot{m} = \frac{4}{3} \frac{c}{\ell} \frac{(P_c - P_e)}{RT} \cdot \frac{1}{\int_0^{\ell} \frac{H}{A^2} dx} \qquad (25)$$

For a conical shape of minimum diameter d, half angle θ, and axial length ℓ, this relation gives

$$\dot{m} = \frac{4}{3} (P_c - P_e) \left(\frac{8\pi}{RT}\right)^{\frac{1}{2}} \left(\frac{1}{2\ell/d}\right) \frac{d}{2} \frac{(d/2 + \ell \tan\theta)^2}{(d + \ell \tan\theta)} \cdot \qquad (26)$$

The flow for other shapes in the free-molecule regime can likewise be calculated from geometric and gas kinetic considerations (cs. refs. 9, 10).

Slip and Transition Flow

For flow in the slip and transition regimes, there exist a few formulae to calculate the flow through orifices and tubes. These are in the form of empirical or semi-empirical corrections to the continuum equations. As an example, consider Poiseuille flow of a gas through a long, straight pipe under the restrictions that (a) the gas is incompressible; (b) the flow is fully developed, i.e., the cross-sectional velocity profile is constant throughout the length; (c) there is no turbulent motion; and (d) the flow velocity at the tube wall is zero. The gas effectively flows in concentric cylinders which slide over each other. Since the flow is steady, the viscous shearing drag on the curved surface is balanced by the pressure. Therefore,

$$2\pi r dx \mu \frac{du}{dr} = -\pi r^2 dP . \tag{27}$$

With the velocity zero at the walls, integration of equation (27) gives

$$u = \frac{d^2 - r^2}{16\mu} \frac{dP}{dx} . \tag{28}$$

The total molecular flow (N) through the tube is

$$N = n \int_0^{d/2} u 2\pi r dr = \frac{\pi d^4}{128 \mu KT} P \frac{dP}{dx} ,$$

and

$$N = \frac{\pi d^4}{128 \mu KT \ell} \left(\frac{P_c^2 - P_e^2}{2} \right) \tag{29}$$

since N is independent of x by conservation of molecules. The mass flow rate is therefore

$$\dot{m} = \frac{\pi d^4}{128} \frac{\bar{P}}{\mu} \frac{\Delta P}{RT\ell} \tag{30}$$

where $\bar{P} = (P_c + P_e)/2$ and $\Delta P = P_c - P_e$.

Although this Poiseuille equation is strictly limited by restrictions given above, it has been modified for use in slip flow. The argument for this is given below. However, since the correction is based on experimental data, it should be pointed out that the modified equation must include a correction for compressibility effects, which are present, even though the argument is based solely on slip.

When the mean free path is smaller than the characteristic dimension, but not negligibly small, an additive term to represent the slip at the surface is used. It is assumed that the gas at the wall has a finite velocity u_o . The number of molecules striking a unit area of wall surface per unit time is

$$N = n\left[u_o + \left(\frac{d^2}{128\mu}\right)\frac{dp}{dx}\right] \quad . \tag{31}$$

An estimate is made for u_o from mean free path considerations. It is found to be

$$u_o = -\frac{2\lambda}{3}\left(\frac{du}{dr}\right)_{r=a} = \frac{2\lambda}{3}\,\frac{d}{4\mu}\,\frac{dp}{dx} \tag{32}$$

where r = cylindrical radial coordinate from the axis of the tube, and x = cylindrical coordinate along the tube. The modified Poiseuille flow equation is (cf. ref. 6)

$$\dot{m} = \frac{\pi d^4}{128\mu RT}\,\bar{P}\,\frac{\Delta P}{\ell} + \frac{\pi d^3}{8c}\,\frac{\Delta P}{\ell} \quad . \tag{33}$$

The additive term has the same form as the free-molecule mass flow through a tube, but is smaller by a factor $3\pi/16$. Equation (33) is valid over a limited range and fails when the mean free path and characteristic dimension are approximately equal.

Dushman gives slip flow formulae for tubes attributed to three sources. From Kennard he gives[11]

$$\dot{m} = \frac{\pi d^4}{128\mu\ell}\,\bar{P}\,\frac{\Delta P}{RT_c}\left(1 + \frac{4\zeta}{a}\right) \tag{34}$$

where ζ is the coefficient of slip given by

$$\zeta = \frac{2-f}{f}\,\frac{\mu}{\bar{P}}\left(\frac{\pi RT_c}{2}\right)^{\frac{1}{2}} \tag{35}$$

and f is the transfer ratio of momentum and represents the fraction of molecular collisions with the walls which result in diffuse scattering of the molecules. The value of f varies between about 0.8 and 1.0 .

Knudsen found that the flow through a long tube can be written

$$\dot{m} = \dot{m}_c + Z\dot{m}_{fm} \tag{36}$$

where $\dot{m}_c$ is the continuum flow rate and $\dot{m}_{fm}$ is the free molecule value. Z is a function of the mean pressure in the tube, the temperature, the tube radius, and the viscosity of the gas.

$$Z = \frac{1 + \frac{d}{\mu}\left(\frac{1}{RT}\right)^{1/2}\overline{P}}{1 + 1.235\,\frac{d}{\mu}\left(\frac{1}{RT}\right)^{1/2}\overline{P}} \tag{37}$$

Sreekanth has recently developed a modified Poiseuille equation from experimental data on the flow through short tubes (ℓ/d from 0.005 to 0.995) at pressure ratios from approximately 1:1 to 30:1 and at Knudsen numbers from 0.1 to 2 (the free-molecule end of the transition regime)[12]. This modified equation is

$$\dot{m} = \left[\frac{\pi d^4}{128\mu RT}\,\overline{P}\,\Delta P + \frac{0.519\,d^3}{\overline{c}}\,\Delta P\right]\frac{1}{\ell(1 + d/\ell)} \tag{38}$$

which is almost identical to the Poiseuille slip flow relation, equation (33), divided by the factor $(1 + d/\ell)$.

The above equations illustrate some of the empirical relations that cover flows in parts of the slip and transition regimes. No known empirical relation or theory covers the entire range from free-molecule to continuum flow.

IV. RESULTS

Experiments were conducted to determine the mass flow through an orifice with an ℓ/d of 0.0895 (Figure 9) at Knudsen numbers of from 8.2 to 0.00068. The pressure ratios across the orifice were at least 100:1 . The experiments were conducted to verify that the low-density gas dynamic facility was functioning properly and that the range from continuum to free-molecule flow could be covered.

The initial set of data, which took one month to collect, revealed that there was a slight leak into the stagnation chamber. The leak rate was approximately one micron-liter per second. This caused the measured flow rates to be too low near and in the free-molecule regime. The measured flow rates dropped to about 85 to 90 per cent of the expected value. This small leak had virtually no effect on the data collected in the continuum regime.

The initial test also revealed some difficulties with the flow measurement system and over-all system stabilization. When the Vol-U-Meter was used for flow measurement, the 1 per cent pressure change in the input to the variable leak when the flow was passed through the Vol-U-meter caused an upset in the steady-state previously attained. This was remedied by throttling the gas in the feed line in parallel with the Vol-U-Meter to match the expected output pressure of the Vol-U-Meter. This meant that no change in feed pressure occurred when the flow was directed through the Vol-U-Meter.

At high Knudsen numbers it was found that it takes as much as five hours for the system to reach steady-state. This is due to the relatively large volumes and small flow rates. After the system stabilizes, it takes about one hour to collect one data point. The system is sensitive to temperature changes, the maximum allowable rate being about $2^{\circ}F/hr$.

As the flow rate increases with decreasing Knudsen number, the time constant of the system decreases and steady-state is attained fairly rapidly -- in as little as fifteen minutes.

After the initial difficulties were remedied, another series of data collecting runs were made. A typical test run is outlined in Appendix I. It is these data that will be discussed in the following sections.

Data Reduction

Two methods were used to reduce the data so that the results could be compared with the results of Liepmann[4] and Sreekanth[12].

Liepmann defines a characteristic velocity, W ; Mach number, Ma ; and Reynolds number, Re ; by

$$W = \left(\frac{P_c - P_e}{\rho_c}\right)^{\frac{1}{2}} \tag{39}$$

$$Ma = \frac{W}{\left(P_c/\rho_c\right)^{\frac{1}{2}}} = \left(\frac{P_c - P_e}{P_c}\right)^{\frac{1}{2}} \tag{40}$$

$$Re = \frac{Wd}{\nu_c} = \frac{d}{\nu_c}\left(\frac{P_c - P_e}{\rho_c}\right)^{\frac{1}{2}} \tag{41}$$

where ν_c is the kinematic viscosity of the gas evaluated at the upstream conditions. He writes the mass flow rate in terms of the orifice area, A , and characteristic velocity, W , in the form

$$\dot{m} = \Gamma \rho_c W A \tag{42}$$

where Γ is a dimensionless function which depends on:

> "Ma , Re , the ratio of specific heats γ , and in the transition region possibly on slip, accomodation coefficients, and possibly a Reynolds number based on the bulk viscosity coefficient. "[4]

The parameter Γ is well defined in the two limits of continuum and free-molecule flow. The free-molecule limit from Knudsen's work is:

$$\Gamma_K = \frac{Ma}{\sqrt{2\pi}} \quad . \tag{43}$$

In the continuum limit with $Ma \doteq 1.0$,

$$\Gamma = \alpha(\gamma) \left[\gamma \left(\frac{\gamma}{\gamma+1} \right)^{\frac{\gamma+1}{\gamma-1}} \right]^{\frac{1}{2}} \tag{44}$$

where $\alpha(\gamma)$ is theoretically well defined, varying from $\alpha = 1$ for a smooth nozzle to approximately $\alpha = 0.85$ for an orifice.

When the Clausing factor ($\varkappa$) is included to modify the free-molecule limit, the relation for Γ becomes

$$\Gamma_K = \frac{\varkappa}{\sqrt{2\pi}} \quad . \tag{45}$$

Liepmann presents his results in the form Γ/Γ_K versus $1/Re$. The continuum limit for the former function is

$$\Gamma/\Gamma_K = \frac{\alpha}{\varkappa} (2\pi\gamma)^{\frac{1}{2}} \left(\frac{2}{\gamma+1} \right)^{\frac{1}{2} \frac{\gamma+1}{\gamma-1}} \quad . \tag{46}$$

Sreekanth presents his results in the form $\dot{m}/\dot{m}_{fm}$ versus Knudsen number defined as the ratio of mean free path evaluated at stagnation chamber conditions to diameter of the orifice or short tube. The expression used to calculate mean free path is[12]

$$\lambda = \left(\frac{16\mu}{5P_c}\right)\left(\frac{RT_c}{2\pi}\right)^{\frac{1}{2}} \quad . \tag{47}$$

As given by equation (24), the free-molecule mass flow limit is

$$\dot{m}_{fm} = \frac{1}{(2\pi RT_c)^{\frac{1}{2}}} A\left(P_c - P_e\right)\varkappa \quad .$$

This means that the continuum limit for the dependent variable is

$$\frac{\dot{m}_c}{\dot{m}_{fm}} = \frac{\alpha}{\varkappa}(2\pi\gamma)^{\frac{1}{2}}\left[\frac{2}{\gamma+1}\right]^{\frac{1}{2}\frac{\gamma+1}{\gamma-1}} \frac{1}{(1 - P_e/P_c)} \quad . \tag{48}$$

In the limit with $P_c >>> P_e$, this reduces to Liepmann's Γ/Γ_K.

It should be noted that the independent variables of Liepmann and Sreekanth are closely related, and in fact differ by a small constant factor in the limit of $P_c >>> P_e$. The ratio Kn to 1/Re is:

$$\frac{Kn}{1/Re} = \left(\frac{16\mu_c}{5P_c}\right)\left(\frac{RT_c}{2\pi}\right)^{\frac{1}{2}} \frac{1}{d}\frac{d}{\mu_c}\rho_c\left(\frac{P_c - P_e}{\rho_c}\right)^{\frac{1}{2}} = \frac{16}{5(2\pi)^{\frac{1}{2}}}\left(1 - \frac{P_e}{P_c}\right). \tag{49}$$

This reduces to 1.275 when $P_c >>> P_e$.

Thus, the two systems of data reduction are similar, but not exactly the same. Both approach the same theoretical limits for continuum and free-molecule flow. The present data were reduced by both of these schemes.

Data Presentation and Analysis

Figure 11 shows the present data superimposed on Liep-

mann's. The two sets conform above $1/Re = 10^{-2}$ and both seem to be slowly approaching the same free-molecule limit of 1.0 . At the lower $1/Re$ end, the two sets seem to be asymptotically approaching different limits. This is as would be expected. The present data were for an orifice with $\ell/d = 0.0895$, while Liepmann's orifice had $\ell/d = 0.0254$. The Clausing factors for the two are, respectively, 0.918 and 0.975.[7] Assuming that $\alpha = 0.85$, the two theoretical values for Γ/Γ_K at the continuum limit are 1.68 and 1.56, respectively. The last few values of Γ/Γ_K obtained from the present data were equal to the theoretical limit of 1.68 . Thus, both sets of data appear to be compatible at both limits and throughout the slip and transition regimes. They both show the same smooth transition from continuum to free-molecule flow.

Between $1/Re = 10^{-2}$ and 10^{-1} , Liepmann's data exhibit a maximum which he attributes to the boundary layer smoothing the entrance condition to the orifice and thereby increasing the mass flow. The present data do not exhibit this maximum, but do exhibit a local maximum or a change in curvature which can be explained qualitatively by the same boundary layer argument.

Figure 12 shows the present data together with Sreekanth's data for an orifice. The similarity between this presentation and Figure 11 is evident. Again, both sets of data are compatible. Sreekanth's data do not extend far enough into the low Knudsen number range to get a good comparison throughout the slip and transition ranges, but a comparison at the free-molecule end shows good agreement.

Sreekanth's empirical formula, equation (38), is also shown in Figure 12. It is satisfactory at the high Knudsen number end of the transition regime. It overestimates the flow rate below a Knudsen number of approximately 0.2 .

Over all, the present data show the transition from continuum to free-molecule flow. The majority of the transition takes place within two orders of magnitude ($0.01 < Kn < 1$, or $100 < Re < 1$). Boundary layer and slip effects seem to be evident in the range $0.001 < Kn < 0.01$, or $1000 < Re < 100$. The slow approach to the free-molecule limit extends beyond $Kn \doteq 10$ or $Re \doteq 0.1$.

V. CONCLUSIONS

The continuous flow, low-density gas dynamic facility designed to study gas flow through various profile apertures in the slip and transition regimes was successfully designed, constructed, and tested. The test was performed with an orifice as the test profile. The data, which exhibit surprisingly little scatter, agree with previous data by Liepmann and Sreekanth. The facility can be used to gather data over a larger range than any previously reported. The range extends from the threshold of free-molecule flow to continuum flow.

The collected data show that the transition to continuum from free-molecule flow takes place in essentially two orders of magnitude in Knudsen number. The transition is smooth, with no discontinuities as would be associated with an abrupt change in the flow field. A comparison of the data with the most recent empirical formulae shows that there is no universal equation to cover the entire spectrum. The measurements show that the flow is approaching the theoretical limits at both high and low Knudsen numbers.

Some interesting questions were raised by this study. The region around Kn = 0.01 or Re = 100 exhibits a local maximum or change in curvature that Liepmann reasoned was caused by boundary layers smoothing the orifice entrance conditions. This area is worthy of a more detailed investigation. The transition to free-molecule flow does not appear to be complete at a Knudsen number of 10. The final approach to the theoretical free-molecule limit appears

to occur very slowly. The final attainment of this theoretical limit also warrants further study.

In conclusion, it can be said that the facility meets its design criteria. It is hoped that it will be used to investigate the areas of orifice flow mentioned above and flows through other profiles such as short tubes and nozzles.

REFERENCES

1. Beckwith, T. G. and Buck, N. L., Mechanical Measurements, Reading, Mass., Addison-Wesley (1961), pp. 376-377.

2. Marble, F. E., "Flow of Gas Through a Nozzle at Very Low Reynolds Numbers," unpublished manuscript, California Institute of Technology and Aeronutronic Division, Philco Corp.

3. Guderley, K. G., Theorie Schallnaher Strömungen, Berlin, Springer-Verlag (1957).

4. Liepmann, H. W., "Gaskinetics and Gasdynamics of Orifice Flow," Journal of Fluid Mechanics, Vol. 10, Part I, (1961), pp. 65-79.

5. Frankl, F. I., Trans. Acad. Sci. USSR, Vol. 58, No. 3 (1947).

6. Present, R. D., Kinetic Theory of Gases, New York, McGraw-Hill (1958), Chapters 2-4.

7. Dushman, Saul, Scientific Foundations of Vacuum Technique, 2nd edition, New York, John Wiley and Sons (1962), Chapters 1 and 2.

8. Knudsen, M., Ann. Physik, Vol. 28 (1909), p. 75.

9. Wu, Yau, "Matrix Probability Theory of Free-Molecule Flow," Rarefied Gas Dynamics, Supplement 1, New York, Academic Press (1961), pp. 141-159.

10. Davis, D. H., Levenson, L. L., and Milleron, N., "Theoretical and Experimental Studies of Molecular Flow through Short Ducts," Rarefied Gas Dynamics, Supplement 1, New York, Academic Press (1961), pp. 99-115.

11. Kennard, E. H., Kinetic Theory of Gases, New York, McGraw-Hill (1936), Chapter 8.

12. Sreekanth, A. K., "An Experimental Investigation of Mass Flow Through Short Circular Tubes in the Transition Flow Regime," Boeing Document D1-82-0427, Boeing Scientific Research Laboratories (1965).

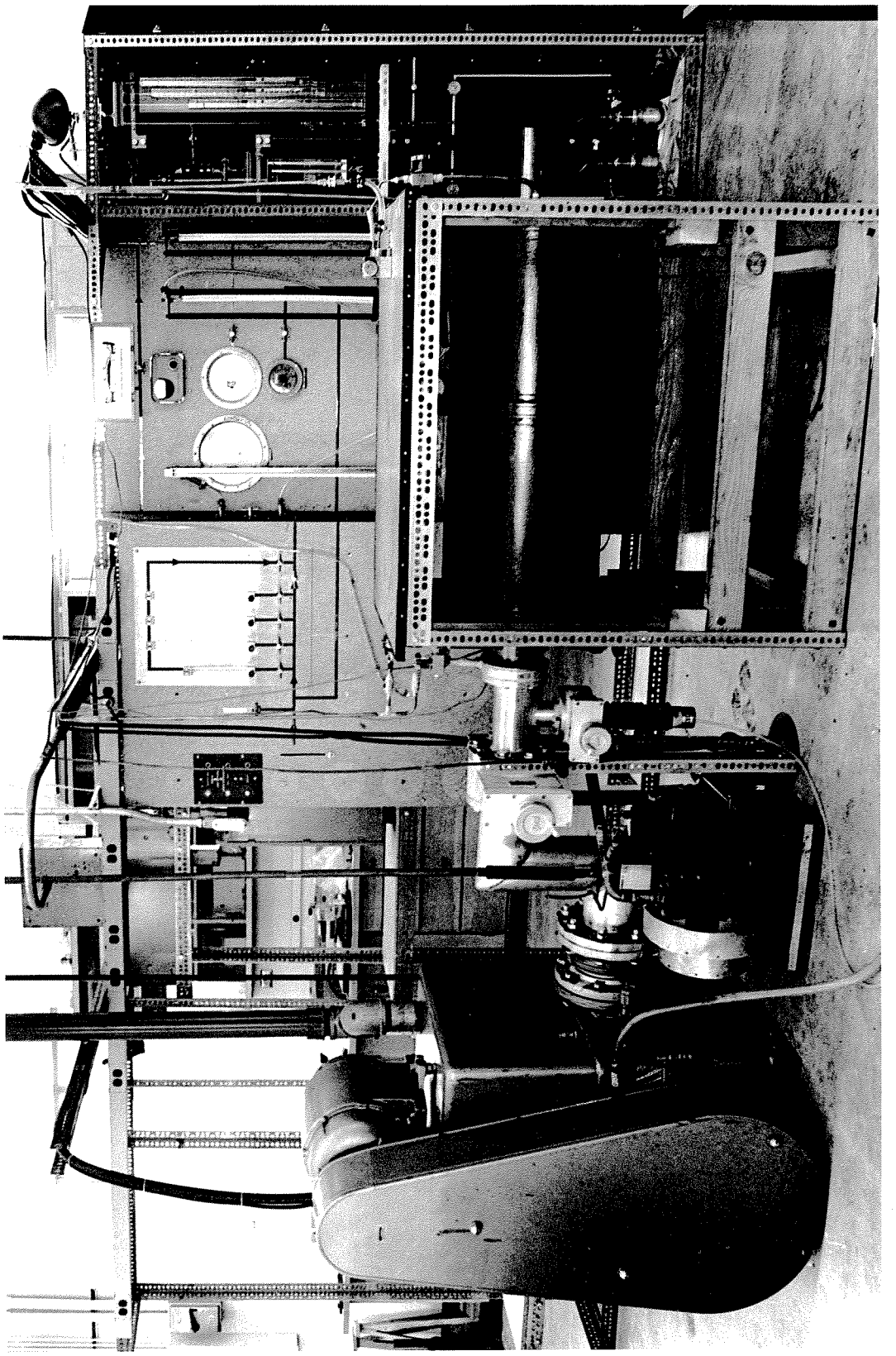

Figure 1. Low Density Gas Dynamic Facility.

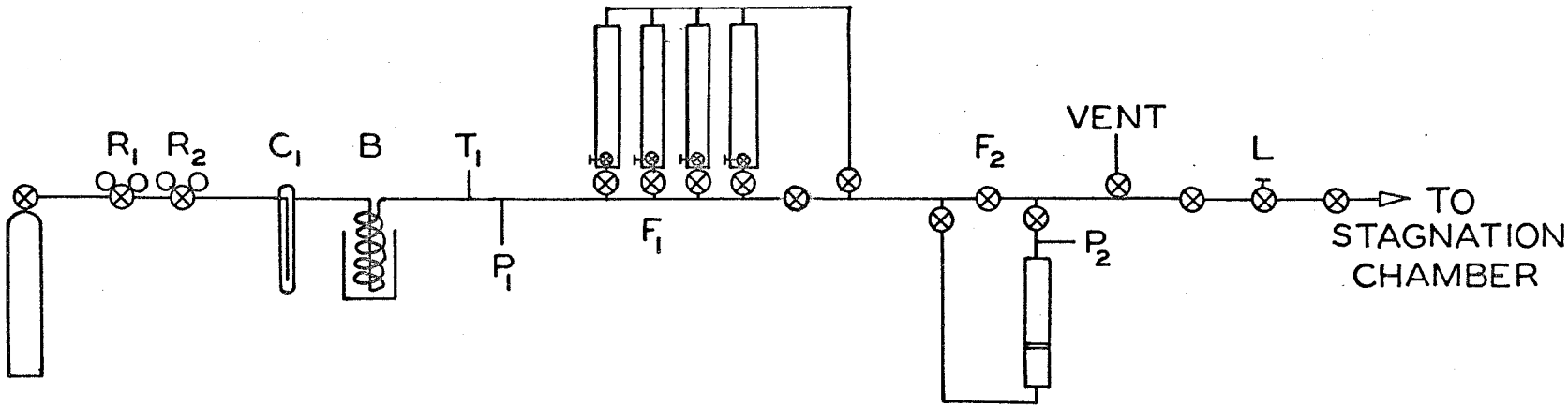

R_1 – HIGH PRESSURE REGULATOR
R_2 – LOW PRESSURE REGULATOR
C_1 – LIQUID NITROGEN TRAP
B – CONSTANT TEMPERATURE BATH
T_1 – TEMPERATURE WELL
P_1 – PRESSURE TAP
F_1 – ROTAMETERS
F_2 – VOL-U-METER
P_2 – PRESSURE TAP
L – VARIABLE LEAK

FIG. 2 GAS FEED AND FLOW MEASUREMENT SYSTEM

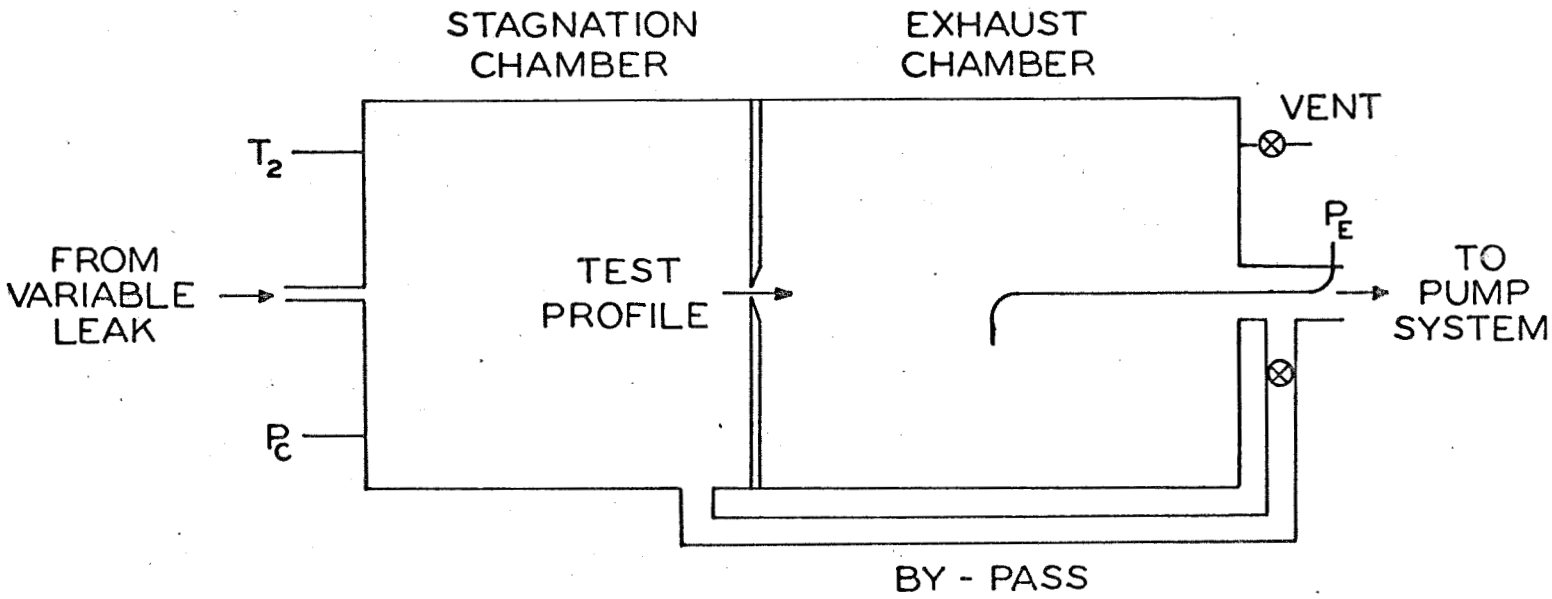

T_2 – TEMPERATURE WELL

P_C – STAGNATION CHAMBER PRESSURE TAP

P_E – EXHAUST CHAMBER PRESSURE TAP

FIG. 3 VACUUM VESSEL SCHEMATIC

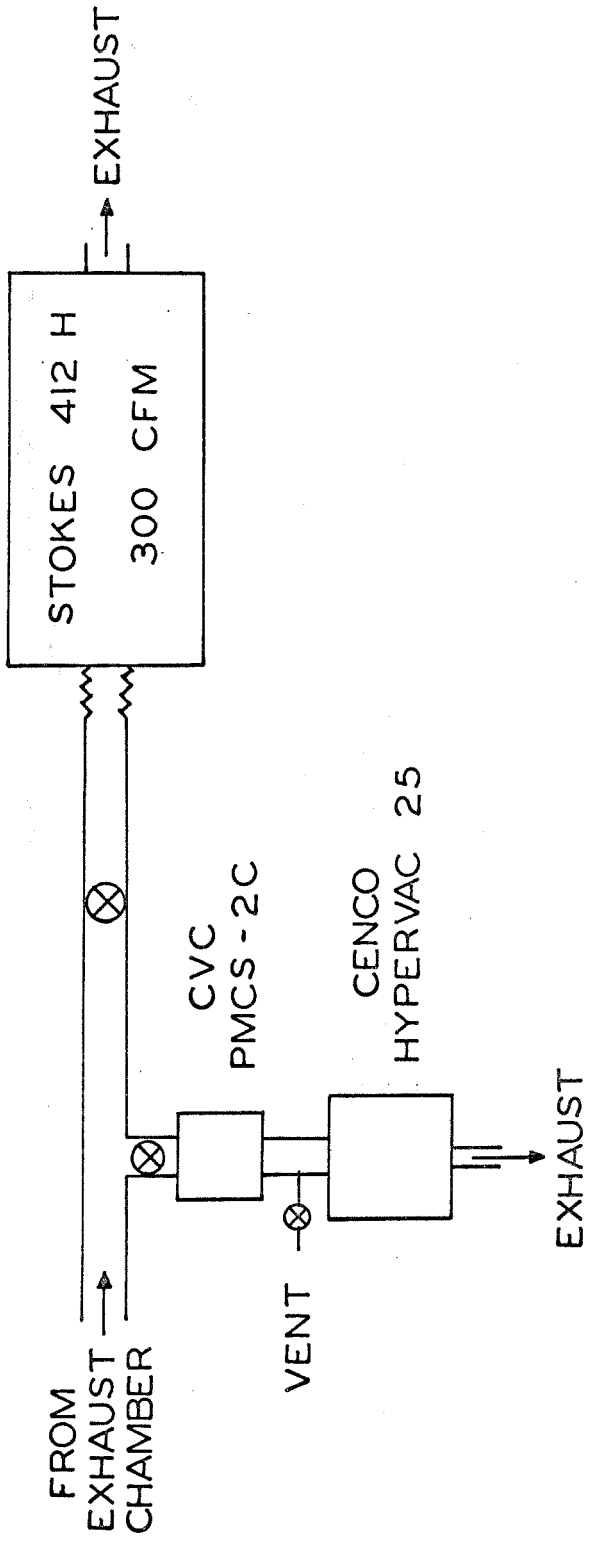

FIG. 4 PUMP SYSTEM SCHEMATIC

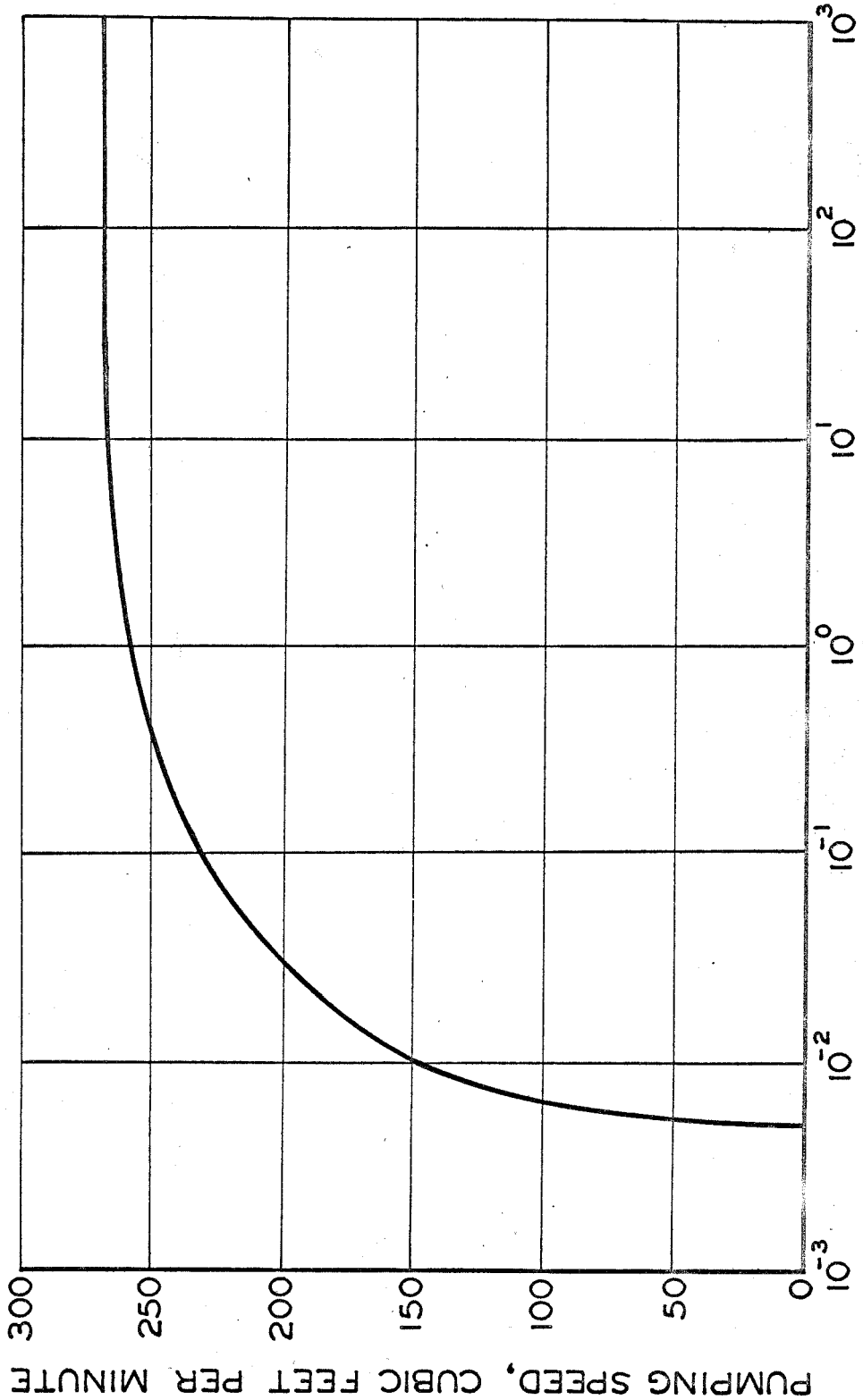

FIG. 5 STOKES 300 CFM DISPLACEMENT, 412-H PUMP

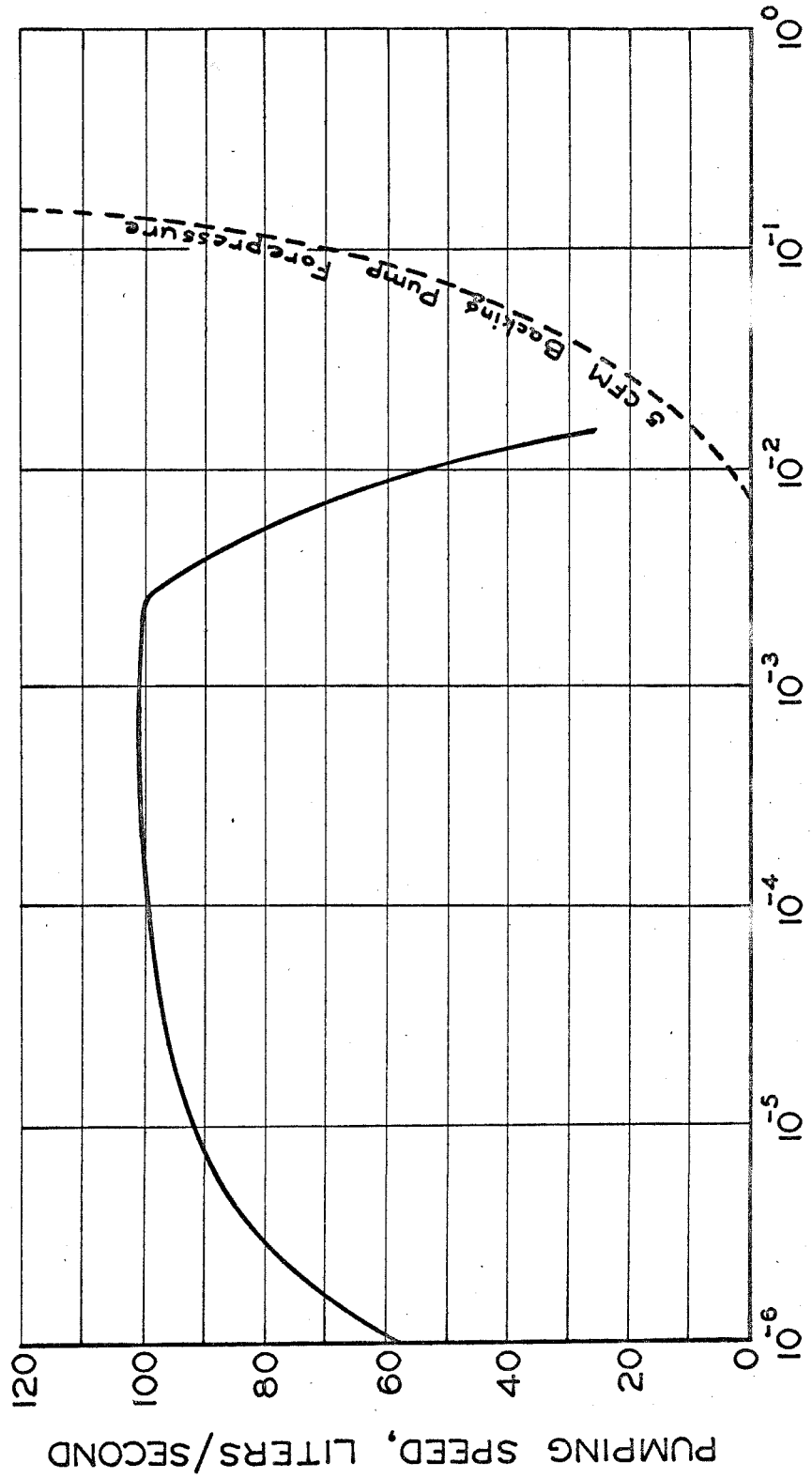

FIG. 6 CVC PMCS-2 FRACTIONATING DIFFUSION PUMP

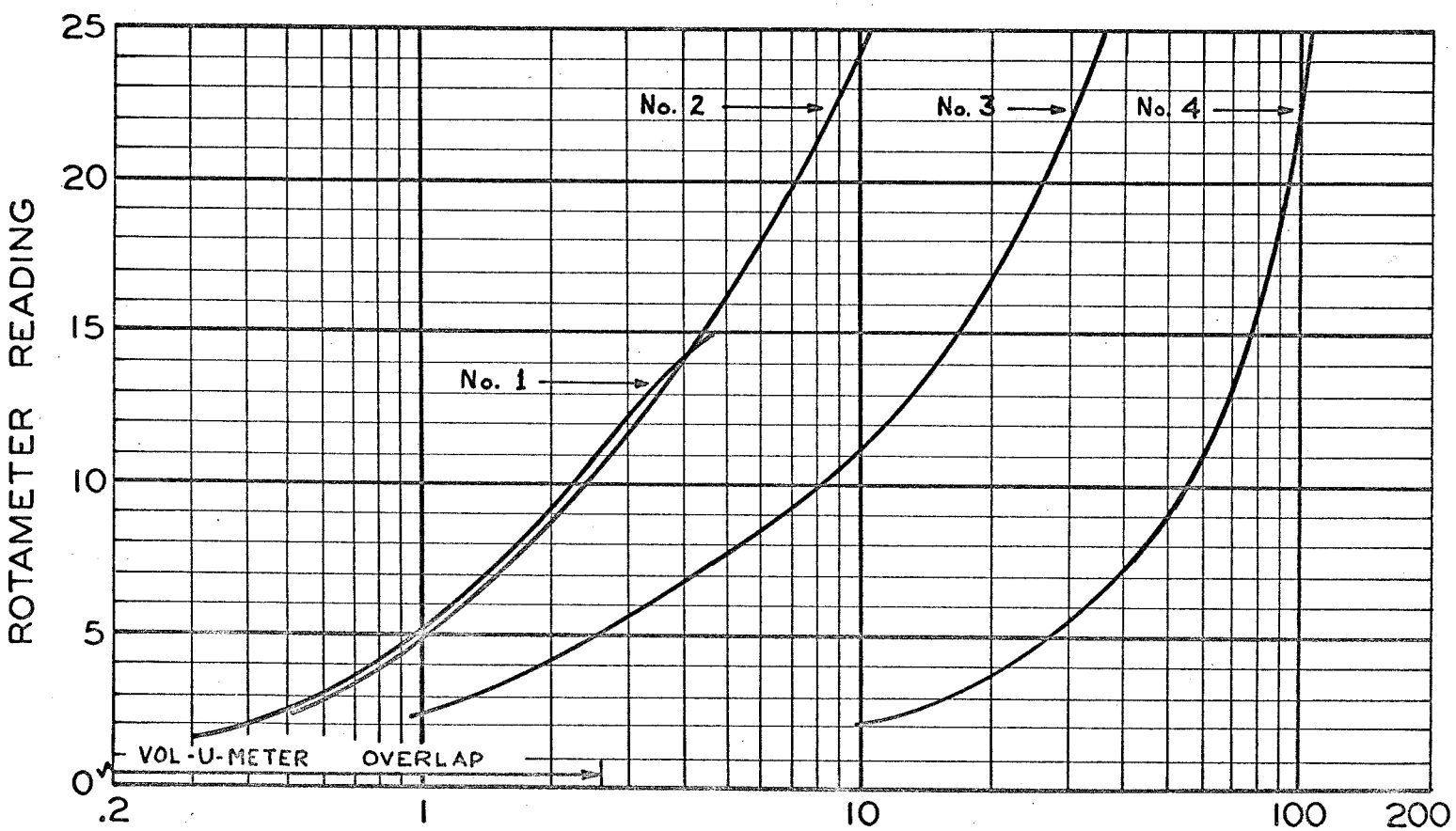

FIG. 7 ROTAMETER RANGES AND OVERLAP

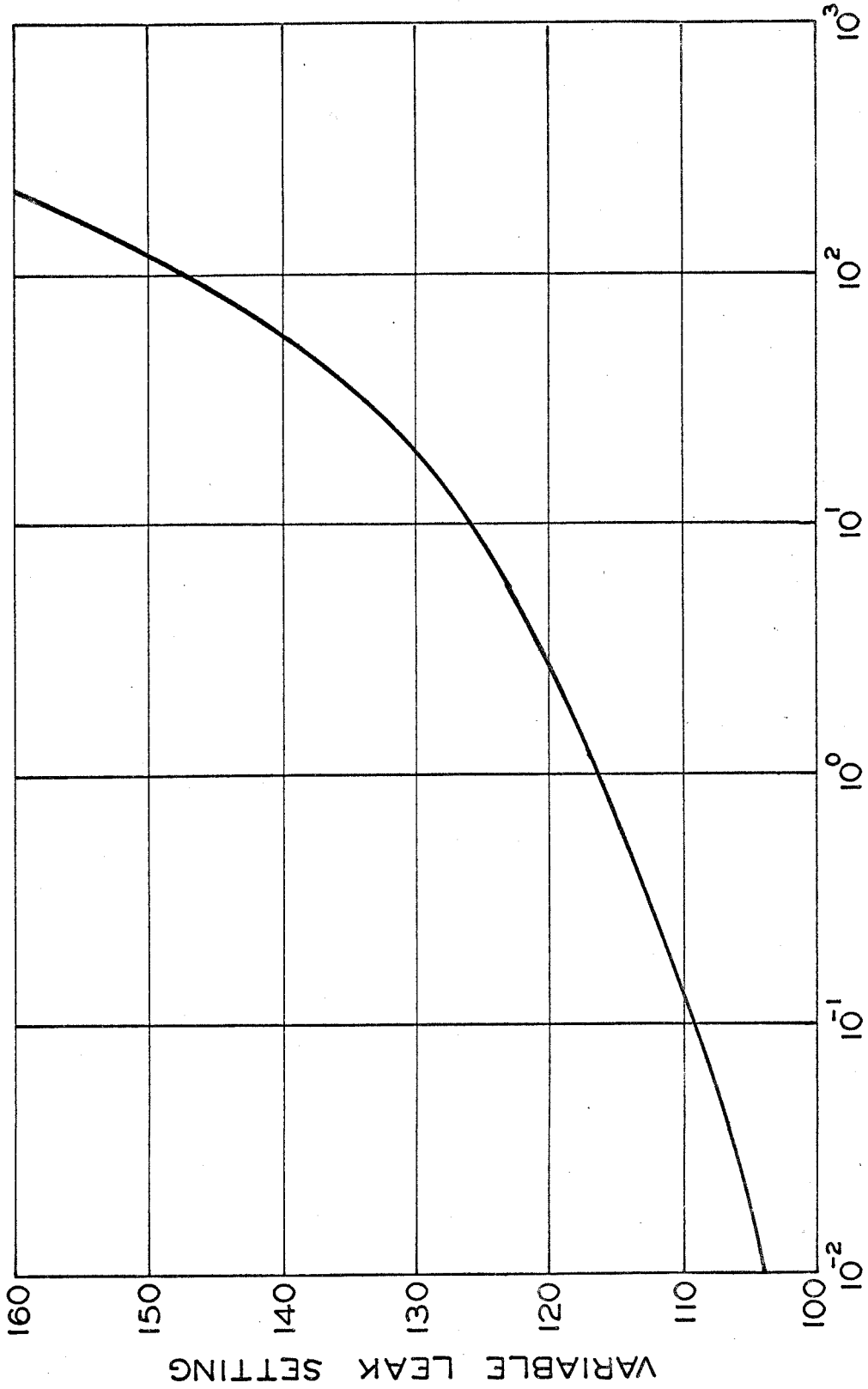

FIG. 8 VARIABLE LEAK SETTING VS. STAGNATION CHAMBER PRESSURE WITH ORIFICE TEST PROFILE

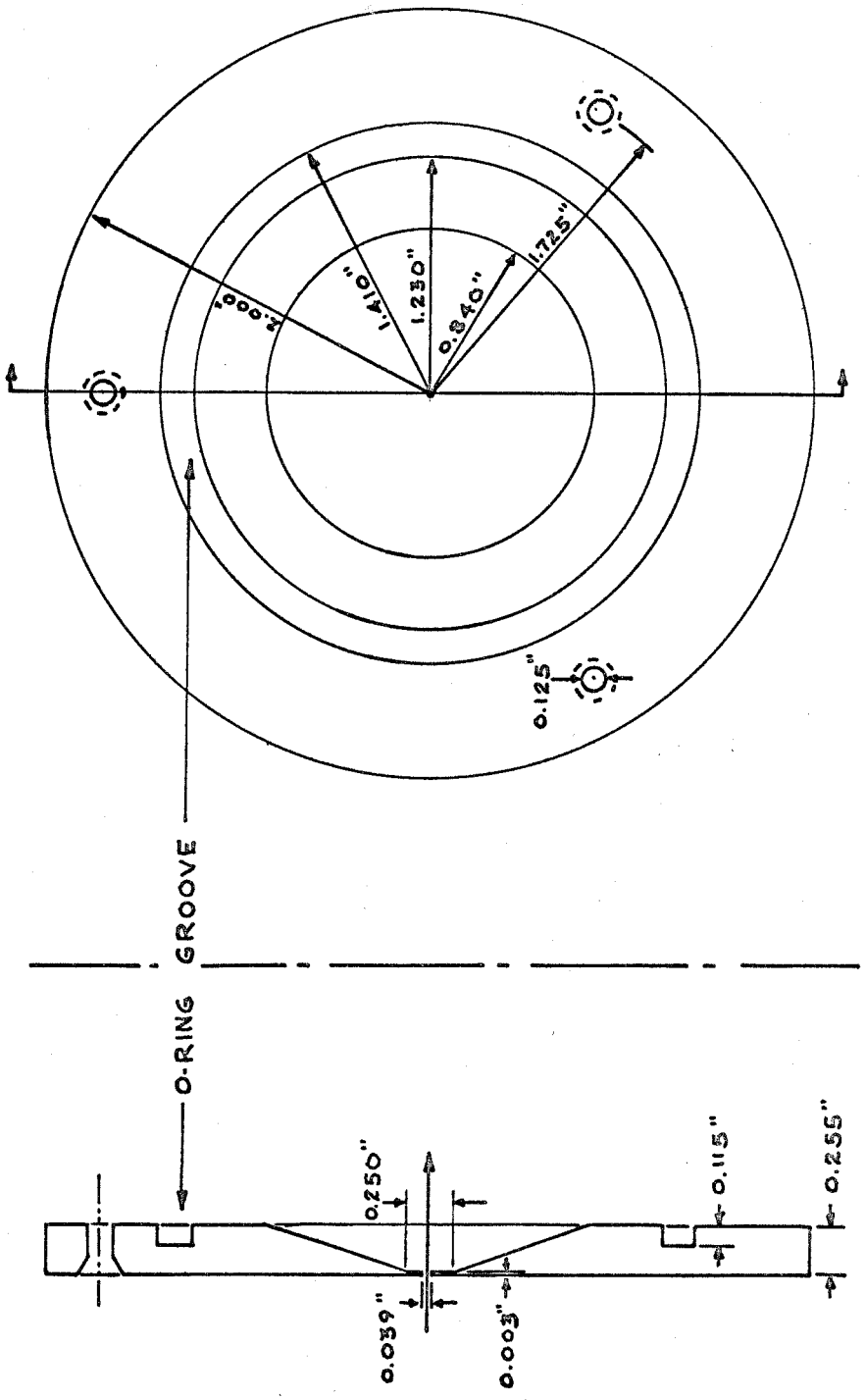

FIG. 9 TYPICAL TEST PROFILE PLATE (ORIFICE)

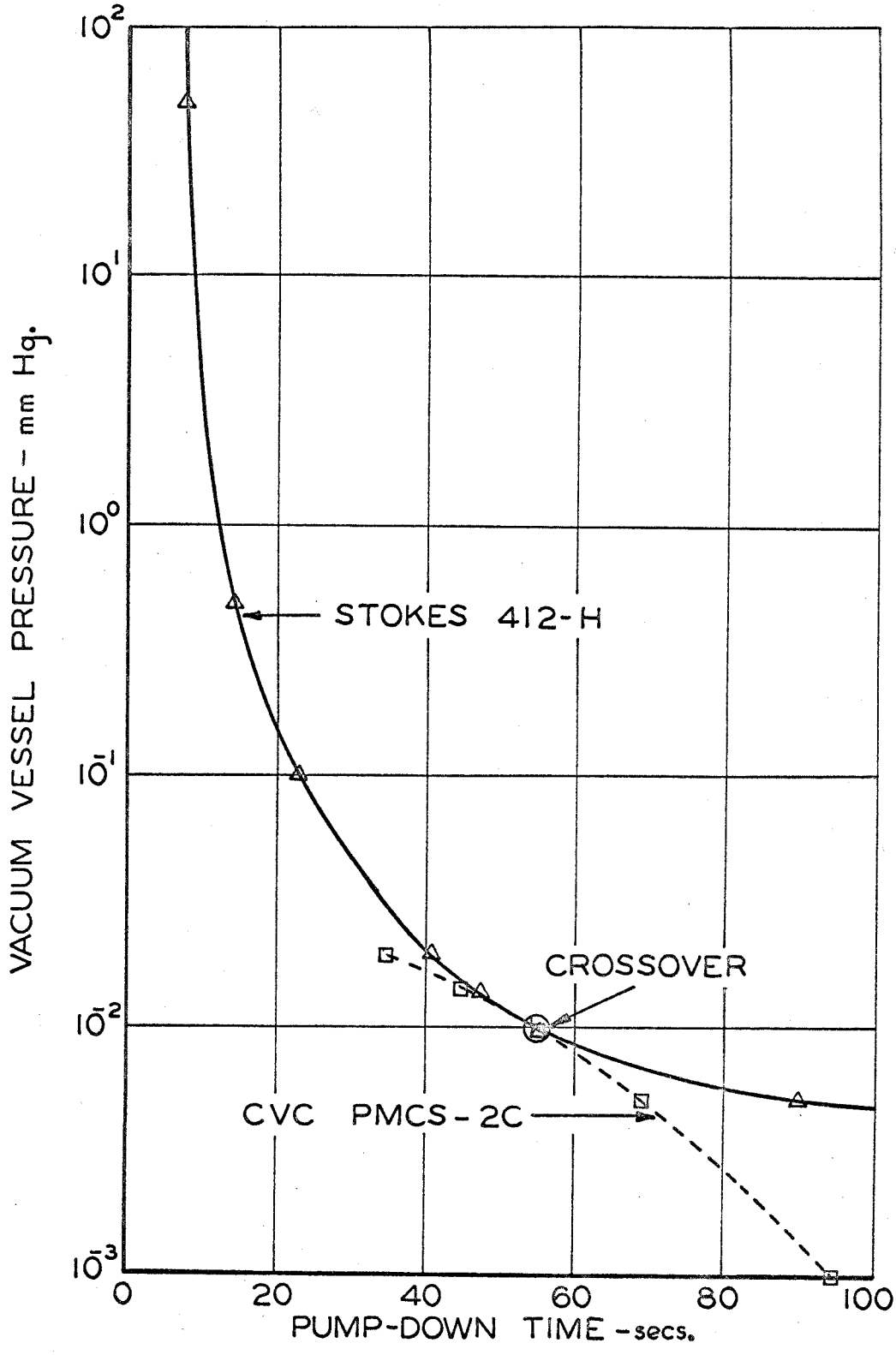

FIG. 10 SYSTEM PUMP-DOWN CHARACTERISTICS

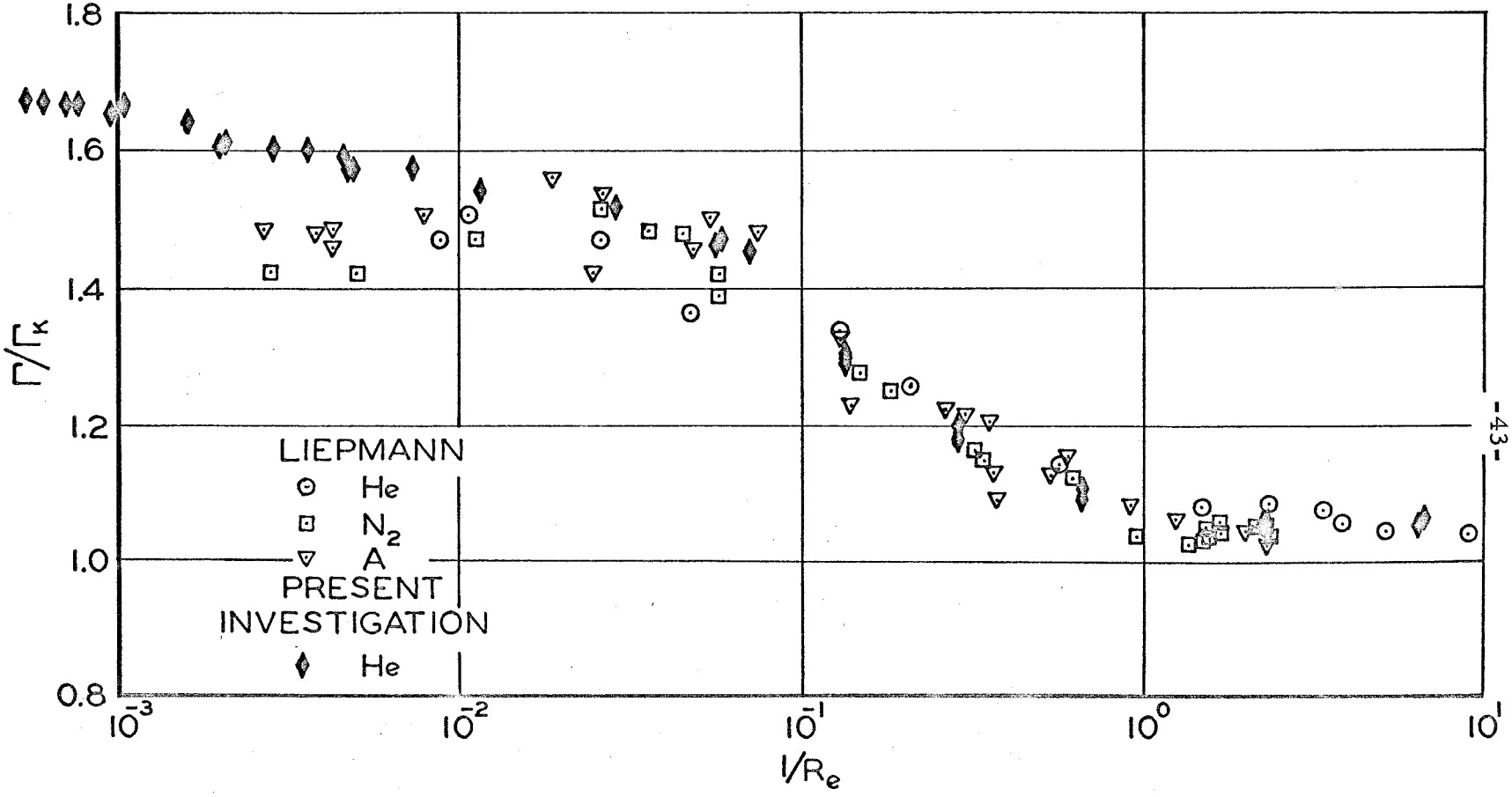

FIG. 11 Γ/Γ_K vs. $1/R_e$; Γ_K IS THE THEORETICAL ASYMTOTIC VALUE OF Γ FOR FREE MOLECULE FLOW

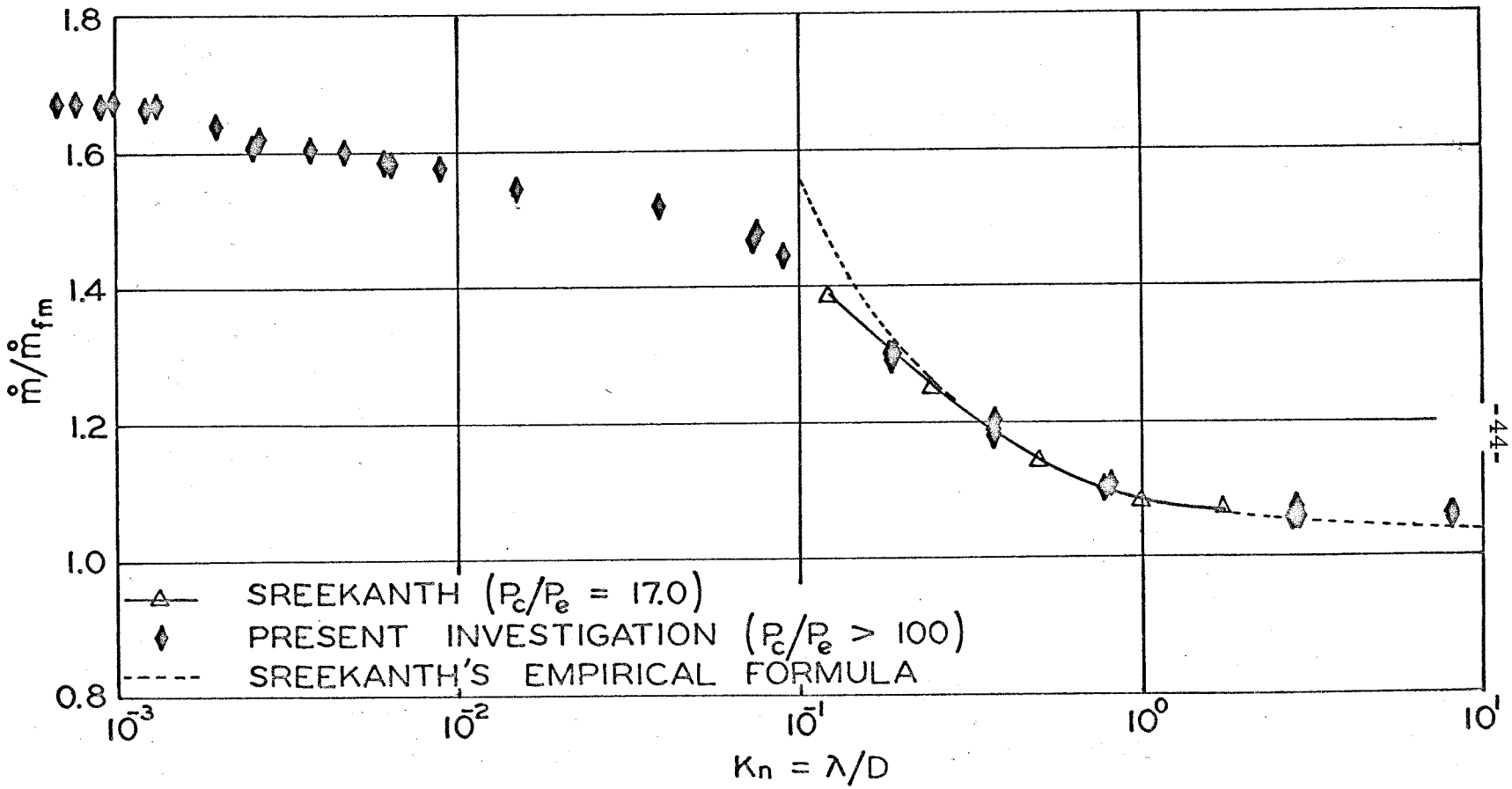

FIG. 12 NONDIMENSIONALIZED MASS FLOW VERSUS KNUDSEN NUMBER

APPENDIX I. Typical Test Procedure

I. Initial Pumpdown

A. Commencing with all valves closed:

1. Open shutoff valves to vacuum pressure measurement lines (3 valves)
2. Open tank bypass valve
3. Open 4" Temescal gate valve

B. Start cooling water flow to:

1. Stokes pump -- approximately 2 gal/min
2. CVC diffusion pump -- approximately 1/15 gal/min

C. Start all pumps:

1. Stokes pump
   a. Check solenoid oil valve with ferromagnetic material
   b. If not magnetized, shut down immediately
2. Cenco Hypervac 25 backing pump
3. CVC diffusion pump

D. Fill McLeod gauge cold-trap reservoir with liquid nitrogen

E. Open McLeod gauge stopcocks

F. Close variable leak to a counter setting of 010.

G. Open shutoff valve downstream of variable leak

H. When exhaust chamber pressure as read by thermistor no. 1 is 10 microns:

1. Close 4" Temescal gate valve
2. Open 2" Temescal gate valve

3. Shut down Stokes pump

I. Pump down system to desired ultimate pressure. Note: if this is the first pumpdown after the system has been exposed to atmospheric conditions:

1. Open Stokes pump gas ballast valves (2)
2. Delete steps D and E
3. Operate on gas ballast for 15 - 20 minutes
4. Close gas ballast before going to Step H
5. Pump down system for at least 24 hours before proceeding (it may be desirable to pump down for a few days to minimize outgassing)
6. Execute steps D and E before proceeding

II. Test Gas Flow Setup

A. Close tank bypass valve

B. Close one of the shutoff valves to the McLeod gauge vacuum line (which one depends on whether exhaust or stagnation chamber pressure is to be measured)

C. Fill feed line cold-trap reservoir with liquid nitrogen

D. Start constant-temperature water bath

1. Start motor and heater
2. Set temperature regulator after flow rate is established

E. Open all valves in the gas feed line except:

1. Close individual rotameter shutoff valves
2. Close rotameter outlet valve
3. Close feed line shutoff valve immediately downstream of the feed line vent valve

F. Open helium (gas supply) bottle

1. Set high-pressure regulator to about 100 psi (must be below 200 psi)
2. Set low-pressure regulator to about 5" H_2O

G. After a few seconds of venting feed gas to the atmosphere:

1. Close feed-line vent valve
2. Open feed-line shutoff valve downstream of the vent

H. Open variable leak to the desired counter reading (graph of approximate counter reading versus stagnation pressure is helpful for this)

1. Monitor exhaust chamber pressure on thermistor no. 1
2. If exhaust chamber pressure exceeds 10 microns, switch pumps
   a. Close 2" Temescal gate valve
   b. Start Stokes pump and wait 30 seconds
   c. Open 4" Temescal gate valve

I. When satisfied with pump setup, monitor stagnation chamber pressure on thermistor no. 2, 0 - 50 mm dial gauge, or manometer. Note: Keep manometer shutoff valve closed below 50 mm Hg to minimize mercury vapor contamination of the variable leak.

III. Flow Rate Measurement

A. Low Flow Rate -- Vol-U-Meter

1. Open input valve to rotameter no. 1
2. Open rotameter output-line shutoff valve

3. Close rotameter bypass valve
4. Partially open rotameter no. 1 needle valve to give about .1 psi pressure drop between flow measurement system input pressure (0 - 15 psia dial gauge) and Vol-U-Meter output pressure (0 - 25, 25 - 50 psia dial gauge)
5. Stabilize system for at least 2 hours
6. Continually refill cold traps
7. Close Vol-U-Meter bypass valve and simultaneously open rotameter bypass valve. Note: this procedure minimizes changes in the gas input pressure to the variable leak when the Vol-U-Meter is thrown into the system.
8. Time the piston between any two volume marks (preferably 0 to 25 cc at the slower rates, and 0 and 22 cc at the faster rates)
9. Before the piston reaches the top of the tube:
   a. Stop the piston by cracking open the Vol-U-Meter bypass valve
   b. Lower the piston gently to the bottom of the tube by carefully opening the Vol-U-Meter bypass valve a bit more

B. Moderate to High Flow Rates -- Rotameters

1. Close input needle valve of desired rotameter
2. Open input valve to rotameter

3. Open rotameter output-line shutoff valve
4. Close rotameter bypass valve
5. Open rotameter input needle valve carefully to full open position. Note: this should be done carefully to prevent damage to the rotameter float.
6. The rotameter can be read continuously and will help indicate when the flow is stabilized (the primary means of assuring stabilization is stagnation chamber pressure measurements).

IV. Other Data Measurements

A. Atmospheric conditions

1. Pressure - barometer (apply temperature/gravity correction to indicated Hg column height)
2. Temperature - thermometer on barometer case

B. Gas inlet conditions

1. Pressure - before flow measurement system
   a. Low-pressure regulator dial gauge (0 - 30 in. H_2O) - this pressure plus atmospheric should equal flow measurement system input pressure
   b. Flow measurement system input dial gauge (0 - 15 psia)
   c. Flow measurement system input manometer (0 - 800 mm Hg gauge)
3. Temperature - before flow measurement system

C. Stagnation Chamber Conditions

1. Pressure

a. Thermistor no. 2

b. McLeod gauges

c. Dial gauge (0 - 50 mm Hg)

d. Manometer (0 - 800 mm Hg) - the scale is already corrected for temperature and gravity - subtract scale reading from corrected barometer reading

2. Temperature - thermometer is in protective shroud protruding from upstream end of tank

D. Exhaust Chamber Conditions - Pressure

1. Thermistor no. 1

2. McLeod gauges

V. McLeod Gauge Operation

A. Activate pressurization system

1. Close individual gauge shutoff valves

2. Open vent line valve

3. Open needle control valve

4. Open nitrogen bottle valve

5. Open regulator shutoff valve

6. Set regulator pressure at approximately 25 psig

7. Close needle control valve

B. Sample measurement

1. Capture of gas sample (either gauge)

a. Close vent line valve

b. Open desired gauge shutoff valve 1 3/4 turns

c. Open needle valve slowly to obtain rate of mercury rise such that sample capture takes 15 - 30 seconds

2. Non-linear gauge

a. After sample capture, increase rate of mercury rise but slow it drastically near the top of the large volume to avoid shocking the closed capillary tube

b. When mercury is in the closed capillary, increase the rate of rise again

c. Slow the mercury rise as the level in the open capillary nears the top

d. Stop the top of the mercury meniscus at the bottom of the black tape line by either closing the needle valve or closing the gauge shutoff valve

e. Tap both capillaries a few times to overcome surface tension effects

f. Read the difference in mercury column heights

3. Linear gauge

a. After sample capture, increase rate of mercury rise but slow it near the top of each large volume to avoid overshooting the compression volume calibration mark

b. Stop the mercury meniscus at the desired scribed volume mark by closing either the gauge shutoff

valve or the needle valve

(1) Use 1st scribe mark and left tube for pressures between 125 and 10 mm

(2) Use 2nd scribe mark and middle tube for pressures between 10 and 1 mm

(3) Use 3rd scribe mark and right tube for pressures between 1 and .1 mm (pressures below .15 mm can also be read on the non-linear McLeod)

c. Read the difference in mercury column heights

4. To lower the mercury level in either gauge:

a. Close needle valve

b. Open vent line valve

c. Open gauge shutoff valve

Note: if a slug of mercury hangs up in the closed capillary of the non-linear gauge, carefully heat the tube with a fuel-rich (yellow) natural gas/oxygen flame until the slug vaporizes.

5. Conversion from scale reading to pressure

a. Apply temperature and gravity correction to all mercury column heights before using scale factors

b. Scale factors

(1) 0 - 100 micron gauge: $P_{(\mu)} = .2375 \times 10^{-2} h_{mm}^{2}$

(2) 0-1 mm gauge: $P_{(mm)} = 1.86 \times 10^{-3} h_{mm}$

(3) 0 - 10 mm gauge: $P_{(mm)} = 1.894 \times 10^{-2} h_{mm}$

(4) 0 - 100 mm gauge: $P_{(mm)} = 2.494 \times 10^{-1} h_{mm}$

VI. System Shutdown

A. Test gas feed

1. Close valve downstream of variable leak
2. Close feed-line shutoff valve downstream of feed line vent
3. Check Vol-U-Meter bypass and rotameter bypass valves open
4. Turn off helium (test gas) bottle
5. Open feed-line vent valve

B. CVC Diffusion pump

1. Close 2" Temescal gate valve
2. Turn off diffusion-pump heater switch
3. Let water and Hypervac 25 run until heater feels cool to the touch
4. Turn off water
5. Turn off Hypervac 25

C. McLeod pressure system

1. Close both McLeod gauge shutoff valves
2. Open vent line valve
3. Turn off nitrogen bottle
4. Open needle control valve

VII. Periodic Checks

A. Check wooden shims under the test-tank support stand twice weekly and knock them back into positions marked on the

floor if vibration has moved them out.

B. Check the oil level in the Hypervac 25 backing pump at least every other day. Add Cenco HyVac oil while pump is running.

C. Oil level in the Stokes 412H pump should be halfway up the sight glass while the pump is running.

D. Temperature of diffusion-pump cooling water taken at the outlet should be 110 - 120 degrees Fahrenheit for maximum pumping rate. Check daily.

E. Stokes pump cooling water should be 70 - 100 degrees Fahrenheit at the outlet. Check during each period of extended operation.

F. Drain the water out of the Stokes pump and refill with clean water twice weekly.